ADVANCED ELECTRONIC MATERIALS
www.advelectronicmat.de

Thin, Skin-Integrated, Stretchable Triboelectric Nanogenerators for Tactile Sensing

Yiming Liu, Lingyun Wang, Ling Zhao, Kuanming Yao, Zhaoqian Xie, Yunlong Zi, and Xinge Yu**

Recent advances in thin, soft skin-integrated electronics have brought many opportunities in the wearable technics. A simple platform with the functionality of self-powering for epidermal electronics is reported. These electronics can generate electricity from external mechanical stresses that associates with triboelectric effect, and therefore afford excellent performance in tactile sensing and energy harvesting. Combined advances in materials and mechanics of the skin-integrated electronics with high efficiency energy harvesting techniques, triboelectric nanogenerators (TENGs) in an epidermal format is realized for the first time. The dots-distributed electrode pattern allows these electronics exhibiting excellent flexibility and stretchability, distinguishing a broad range of pressures that are relevant to normal body motions. The electricity output of the epidermal device from simple finger tapping modes can achieve >60 V of voltage and >1 μA of current, which is sufficient to light up 15 small light-emitting diodes. Furthermore, the authors also report a 4 × 4 sensor array based on these TENGs, and demonstrate a skin-like electronics for real-time motion monitoring and tactile mapping.

1. Introduction

Thin, soft, stretchable sensors have attracted great attention around the world, due to their advantages of high flexibility, multi-functions, and bio-integration/compatibility.[1–6] In recent years, many research efforts have been focused on developing functional materials[7–11] and designing advanced device structures[12–17] to expand the applications of the flexible sensors. For instance, soft materials with great electrical properties, fancy electronic interconnects based on serpentine, island-bridge, and nano-mesh enable superior flexibility for wearable electronics.[18–21] To realize a portable platform of wearable electronics, developing self-power flexible sensors have become a trend.[22–27] Currently, self-powered technologies based on piezoelectric materials[28–32] and triboelectric nanogenerator[33–37] are two typical strategies to convert mechanical energy into electricity. Compared to piezoelectric nanogenerator, triboelectric nanogenerator is more suitable for energy harvesting, as it typically can provide much higher output voltage and current.[38–40] However, reports of using triboelectric nanogenerator for flexible sensors are still much less than those of piezoelectric based ones.[41] The typical method of using triboelectric nanogenerator for stress sensing involves difference of electrical signal output with different contact areas.[35,42,43] Therefore, human motion caused contact separations in the wearable triboelectric nanogenerator can result in electricity output and thus tactile sensing.[35] To better meet the requirement of skin integration, it is accessible to fabricate ultrathin single-electrode mode based triboelectric nanogenerator by decreasing the thickness of encapsulation layers (Figure S1, Supporting Information).

Here, we introduce an ultrathin, stretchable triboelectric nanogenerator based epidermal electronics for tactile sensing and energy harvesting. The device adopts a single-electrode mode that includes copper (Cu) traces with two layers of soft polydimethylsiloxane (PDMS) as the substrate and encapsulation and triboelectric negative material. The simple geometry design enables energy conversion from mechanical stress to electrical signals, and can easily be extended to larger or smaller devices to address requirement in tactile sensing and energy harvesting. A tactile sensing array with 4 × 4 generators was demonstrated and showed great sensitivity and selectivity to various kinds of touching modes. The ability to characterize specific mechanical stress and generate electricity from various body activities is of broad potential interest to the wearable electronics.

2. Results and Discussion

Figure 1a illustrates the schematic diagram of the epidermal electronics, where the 170 μm thick PDMS serves as both the supporting substrate (20:1; ≈500 kPa) and top triboelectric layer (10:1; ≈1 MPa) for simplifying the fabrication process, and Cr/Cu (10 nm/200 nm) with polyimide (PI, 2 μm)

Y. Liu, L. Zhao, K. Yao, Dr. Z. Xie, Dr. X. Yu
Department of Biomedical Engineering
City University of Hong Kong
Hong Kong 999077, P. R. China
E-mail: xingeyu@cityu.edu.hk
Dr. L. Wang, Dr. Y. Zi
Department of Mechanical and Automation Engineering
Chinese University of Hong Kong
Hong Kong 999077, P. R. China
E-mail: ylzi@cuhk.edu.hk
The ORCID identification number(s) for the author(s) of this article can be found under https://doi.org/10.1002/aelm.201901174.

DOI: 10.1002/aelm.201901174

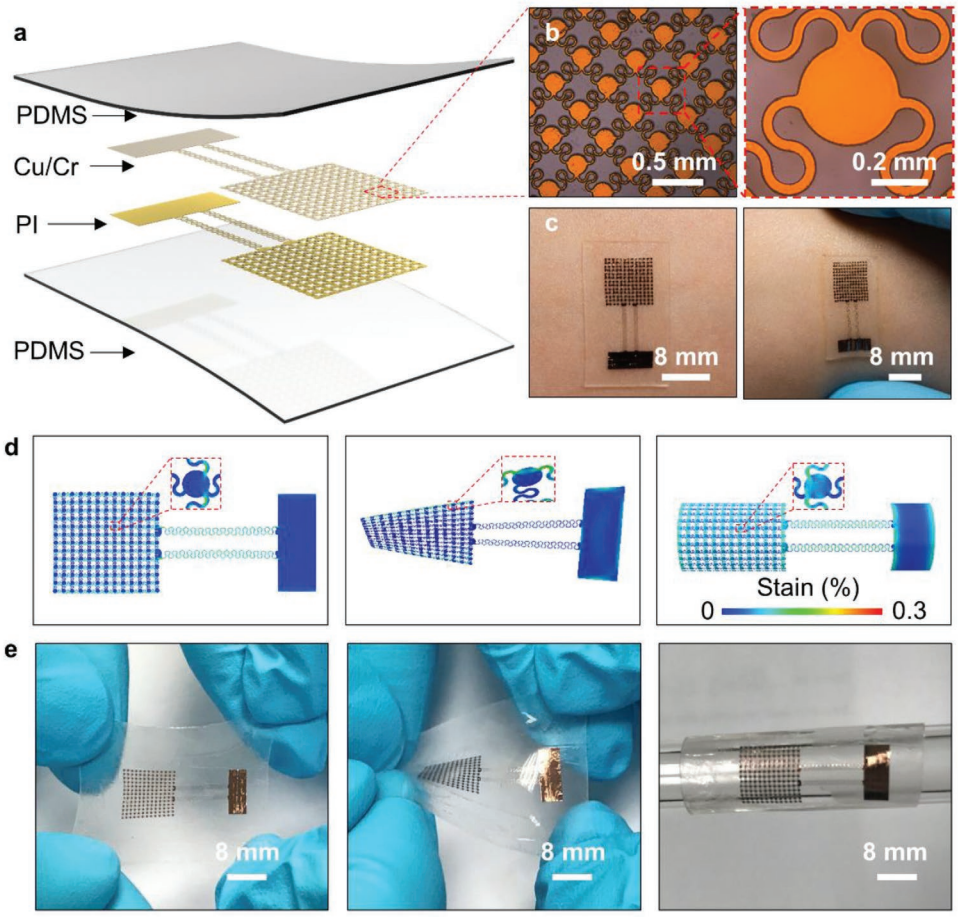

Figure 1. Stretchable and ultrathin triboelectric nanogenerator based on single-electrode working mode. a) Schematic illustration of a skin-integrated triboelectric nanogenerator. b) Optical image of patterned copper electrode design with PI supporting layer, and the enlarged optical image of the electrode. c) Optical images of the triboelectric nanogenerator mounted on the surface of human arm, and deformations together with skin. d,e) FEA results of strain distribution and optical images of the nanogenerator under stretching, twisting, and bending.

supporting layers patterned with serpentine connected discs act as electrodes. PDMS is a widely used material in flexible electronics and bio-integrated electronics because of its good biocompatibility, physical/chemical stability, and excellent stretchability.[44] Moreover, its electrical negative nature allows the use in triboelectric nanogenerator as an electrification layer.[45] Therefore, the top PDMS layer and human skin work as the triboelectric negative and positive materials, respectively.[46,47] When any touching happens on the PDMS layer by human body, such as fingers, electrons would inject from the skin into PDMS, and leave skin positively charged and PDMS negatively charged (Figure S2, Supporting Information). An electrical potential difference is established when the skin moves away from the PDMS,[48] and electrons in the electrode are induced by the negative charges on PDMS layer, emerging from the upper interface between PDMS and electrode. Figure 1b shows the serpentine connected discs patterned chromium/copper electrode, where the thin PI layer underneath provides electrical insulation and mechanical strain isolation. The light weight (≈0.25 g) and small size (19 mm × 8 mm × 0.35 mm) of the device allow for skin integration on different parts of the body.

Figure 1c and Figure S3, Supporting Information present a typical scenario of use-case that involves mounting the soft device onto the skin. The conformal coating of the device allows consistent deformation with skin stretching and acts as a temporary tattoo. Therefore, the resulting soft device can directly couple to the skin at different body locations by van der Waals forces alone (Movie S1, Supporting Information and Figures S4 and S5, Supporting Information). The finite element analysis (FEA) guided the design of the electrode geometries and entire device layout to minimize the strain in the Cu layer under typical deformations (commercial software ABAQUS, 2016). Additionally, all the layers were perfectly bonded together in FEA. The simulated strain distribution in the Cu traces and corresponding optical images for a representative device are shown in Figure 1d,e (more mechanical deformations in Figure S6, Supporting Information). The maximum principal strains in the Cu traces remain below the yield stain (0.3%) for the device under ≈8% stretching, 76° twisting, and bending with a radius of 5 mm. These results highlight the range of robust and elastic responses, which is necessary to accommodate realistic physiological motions.

According to the designing strategies of triboelectric nanogenerators, the induced voltage and current depend on the

magnitude of the difference in electronegativity between dissimilar functional materials[49] and contact behaviors between triboelectric layers.[50] So, the thickness and stiffness of the PDMS top triboelectric layer were studied and optimized by tuning processing parameters and the crosslink weight ratios. Stable mechanical forces driven by an oscillator controlled electromagnetism hitting setup were used to characterize the response of electrical signals to external forces. **Figure 2**a,b show the open-circuit voltage and short-circuit current as functions of different PDMS thickness, where the external force was set at 14.5 kPa and frequency of 1 Hz. It is obvious that the output signals decreased with the increase of PDMS film thickness, indicating thinner triboelectric PDMS layers are favorable for energy harvesting. The output electrical signal achieved the maximum value when PDMS thickness was 0.17 mm, with a corresponding open-circuit voltage of 5.76 V and short-circuit current of 0.16 μA, respectively. While the open-circuit voltage and short-circuit current of the device with 1 mm thick PDMS layer were only 2.53 V and 0.09 μA. Stiffness studies involve changing the weight ratio of the crosslink and fix the thickness of 0.17 mm. PDMS with four different weight ratios of crosslink of 1:5, 1:10, 1:15, and 1: 20 was used as top layer in the devices. Figure 2c,d show the open-circuit voltage and short-circuit current as a function of PDMS with different stiffness (stress of 14.5 kPa and frequency of 1 Hz). As the stiffness increases, both output voltage and current increase in a nearly linear manner, where the device with ratio of 1:5 exhibits the highest output of 6.44 V and 0.17 μA. Soft PDMS is stickier than metal electrode, thus results in difficulty of separation between the metal and negative (PDMS) triboelectric layers. However, silicone with low modulus is the basic requirement for flexible and stretchable electronics. Here we chose PDMS with 1:10 crosslink weight ratio as the top triboelectric layer based on the following two considerations: i) Comparable electrical signal output (voltage of 5.76 V, and current of 0.16 μA) to the best device; ii) Acceptable modulus for flexible electronics (see the FEA information on page 2 for detail).

Figure 2e,f shows the open-circuit voltage and short-circuit current as a function of frequency at a constant stress of 3 kPa. The output voltages of the device were ≈2.20, 2.61, 2.89, 3.03, 3.23, and 3.80 V under the frequencies 1, 3, 5, 7, 9, and 15 Hz, respectively. The output currents were 86, 92, 97, 96, 98, and 100 nA under the frequencies 1, 3, 5, 7, 9, and 15 Hz, respectively. Obviously, the open-circuit voltage and short-circuit current increased with the increasing of frequency at a constant stress. Here the frequency-dependent behavior of the output electrical signals is due to the low impedance of the measured instrument (more details in Section 4).[51] Figure 2g,h

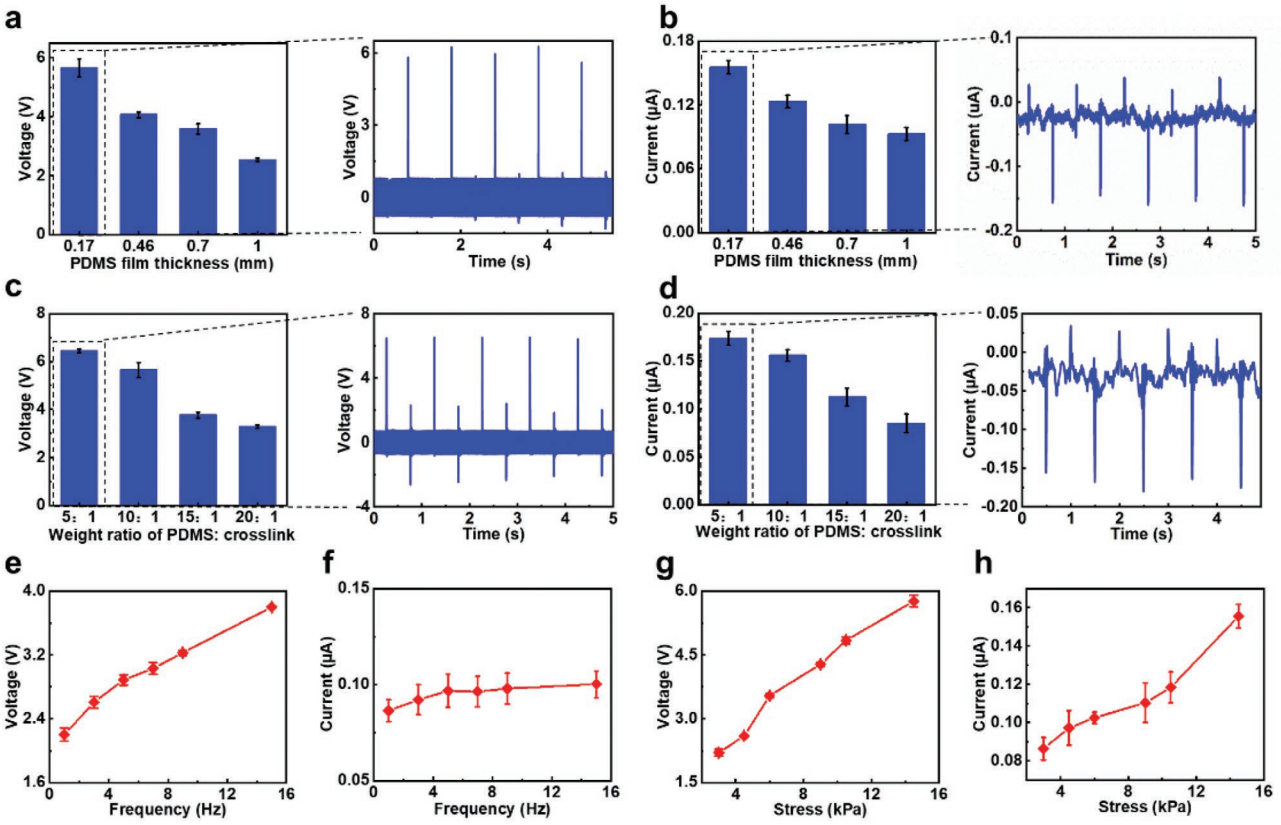

Figure 2. The electrical characteristics of the TENG. a) The open-circuit voltage and b) short-circuit current by nanogenerator as a function of triboelectric PDMS layer thickness when weight ratio of crosslink:PDMS = 1:10. c) The open-circuit voltage and d) short-circuit current by nanogenerator as a function of crosslink weight ratio in triboelectric PDMS when thickness of PDMS layer is 0.17 mm. e) The open-circuit voltage and f) short-circuit current by nanogenerator as a function of frequency at a constant stress of 3 kPa when the PDMS (crosslink:PDMS = 1:10) layer has a thickness of 0.17 mm. g) The open-circuit voltage and h) short-circuit current by nanogenerator as a function of stress at a constant frequency of 1 Hz when the PDMS (crosslink:PDMS = 1:10) layer has a thickness of 0.17 mm.

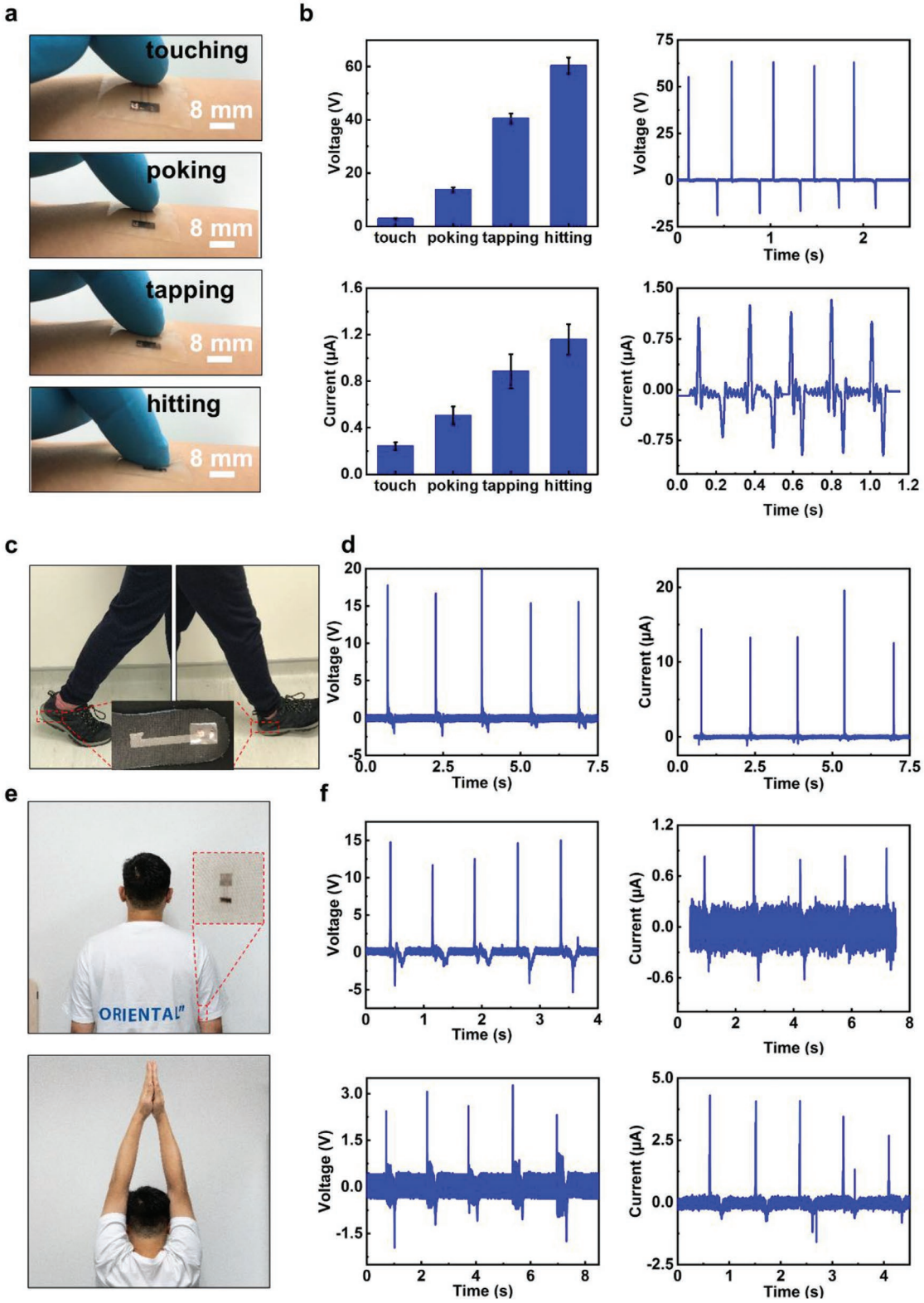

Figure 3. The output signals of the triboelectric nanogenerator under different external loads. a) Optical images illustrating four different external loads on the nanogenerator attached onto the surface of human arm, touching, poking, tapping, and hitting. b) The open-circuit voltage and short-circuit current produced by triboelectric nanogenerator under the four external force shown in (a). c) Optical images presenting human walking as nanogenerator was attached onto insole (see the inset). d) Electrical response of nanogenerator to human walking shown in (c). e) Optical images showing human exercising motion as nanogenerator was attached to the gusset. f) Electrical responses of nanogenerator to two exercising modes, slow and fast.

summarizes the open-circuit voltage and short-circuit current of the triboelectric nanogenerator as a function of applied stress at a constant frequency (1 Hz). Both the output voltage and current increased in a linear manner along with the external force, where the voltage and current increased from 2.2 V and 86 nA under 3 kPa to 5.76 V and 156 nA under 14.5 kPa. These results suggest that the triboelectric nanogenerator are distinguishable for different magnitudes and frequencies of the external force. Figure S6, Supporting Information demonstrated the stability of the triboelectric nanogenerator under a constant stress and frequency of 9 kPa and 5 Hz for over 2000 cycles.

Various external forces applied to the generator by finger touching, poking, tapping, and hitting yield corresponding responses that associate with different output voltage and current (**Figure 3**a). The open-circuit voltage and short-circuit current of the generator varying from 2.78 V/0.24 μA to 60.4 V/1.16 μA were observed for the above-mentioned touching modes. These results are consistent with the results shown in Figure 2e. The pressure of gentle touching is ≈2.5 kPa, poking is ≈12.5 kPa, tapping is ≈37.5 kPa, and hitting is ≈ 59.8 kPa. The extremely high voltage and current output induced by finger hitting can even light up over 15 LEDs (see Movie S2, Supporting Information). To further demonstrate their energy harvesting ability, the soft devices were integrated with an insole and a gusset (Figure 3c–e). When the device was mounted onto an insole, contact and separation will happen alternately between the skin and the PDMS during walking and running. Due to the great stretchability and ultrathin thickness, the electronics can stand large mechanical deformations of the insole without causing any damage during walking and running. As shown in Figure 3d, the high voltage and current output (16.75 V and 14.33 μA) indicate its potential in charging capacitors, lighting up small LEDs and other related energy harvesting. Similarly, the electronics can be mounted on a gusset and collect electricity from daily human activities (Figure 3e). To illustrate the influence of exercising frequency on the signal output of the electronics, the examiner swung an arm under two different frequencies at a constant arm swinging amplitude. Consistent with the results in Figure 2e,f, higher frequency activity could induce higher voltage and current.

Next, a 4 × 4 tactile sensing array included 16 triboelectric devices as sensing units was demonstrated for electric skin applications (**Figure 4**a). The array device shares the same layout of the single triboelectric nanogenerator that is shown in Figure 1a, consisting of a thin metal functional layer and two PDMS layers. The overall size of the ultrathin device is 75 × 50 × 0.35 mm^3, allows incorporation with human skin without any irritation (Figure 4b), and exhibits excellent flexibility and stretchability (Figure 4c and Figure S8, Supporting Information). After continuous stretching, twisting, and bending, the device still operated as usual, indicating the robust stability and durability for extreme mechanical deformations. Furthermore, the device was very sensitive to finger touching with clear voltage and current response, affording the skin-like platform with capabilities of rebuilding the tactile information. Figure 4d,e presents the voltage response of the device to a finger written "CITYU" pattern. The finger slide induced

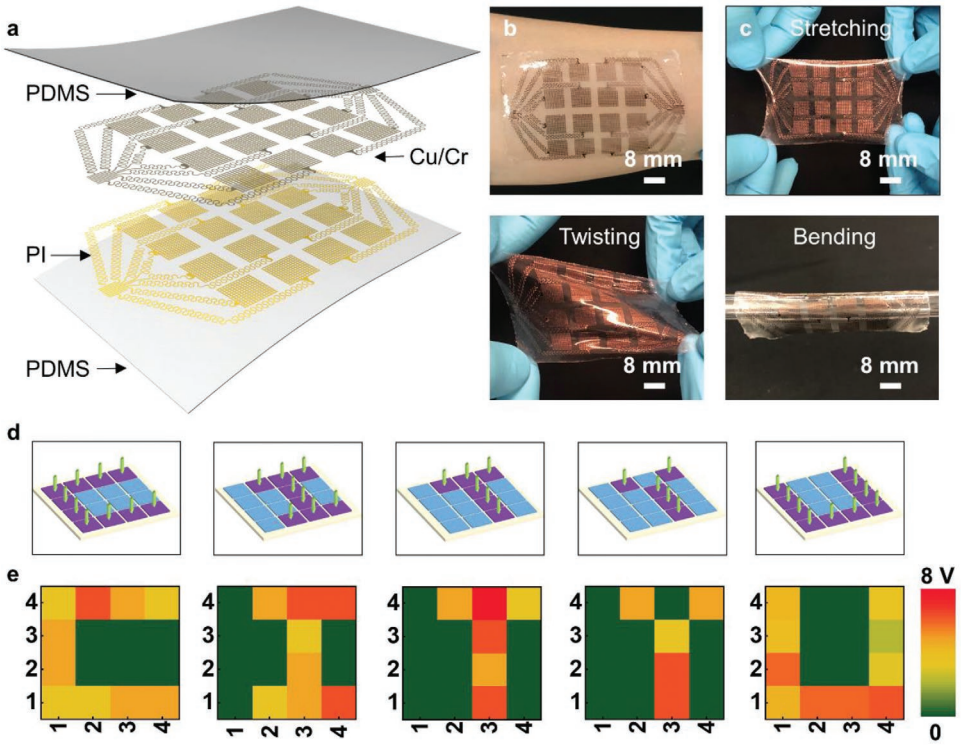

Figure 4. A skin-integrated 4 × 4 arrayed triboelectric tactile sensor. a) Schematic illustration of the 4 × 4 arrayed tactile sensor. b) Optical image of the arrayed sensor mounted on the surface of human skin. c) Optical images of the arrayed sensor under three mechanical deformations, including stretching, twisting, and bending. d,e) The positions of external force on the arrayed sensor, and their corresponding electrical responses.

voltage on the sensors ranged from 2 to 8 V, which is great enough for direct use without further signal amplification.

3. Conclusion

In summary, the results presented here demonstrate the basis for a simple and effective route for self-powered skin electronics, which associates with ultrathin soft triboelectric nanogenerator for tactile sensing and energy harvesting. Characterizations on a range of frequencies and pressures prove the great sensitivity of the device as sensors and excellent energy conversion capability of the device as energy harvesters. These and many other opportunities, taken in the context of the advantages of the triboelectric nanogenerator as a point of skin-integrated electronics, demonstrate many bright futures and applications for self-powered wearable electronics and many other related fields.

4. Experimental Section

Assembly of the Triboelectric Nanogenerator: The schematic illustration of the assembling process is shown in Figure S9, Supporting Information. First, a quartz glass was cleaned with acetone, ethanol, and deionized water (DI water), sequentially. Then, PMMA solution (20 mg mL^{-1}) was spin-coated onto the surface of the cleaned glass at 2000 rpm for 30 s, and then baked on the hotplate at 200 °C for 20 min. The PMMA thin film served as a sacrificial layer. Afterward, poly-amic acid solution (12.0 wt% ± 0.5 wt%, 3 um) was spin-coated on the PMMA sacrificial layer at 3000 rpm for 30 s. Then, the PI thin film was cured on the hotplate at 250 °C for 30 min to densify. Cr (10 nm) and Cu (200 nm) were next deposited on the PI film by magnetron sputtering, and then patterned with photolithography and further wet etched to form the desired pattern. The photolithography process was carried out by exposure of the pre-spin-coated (3000 rpm, 30 s) and soft baked (110 °C, 3 min) positive photoresist (PR, AZ 5214, AZ Electronic Materials) to the ultraviolet light for 5 s. The pattern was then developed in AZ 300MIF developer for 15 s and followed with a post bake at 110 °C for 3 min. After etching the Cu/Cr layer, the PR was removed with acetone, and rinsed with DI water. A second layer of PI thin film (2 µm) was then spin-coated (3000 rpm, 30 s) and annealed (250 °C, 30 min), followed by selectively dry etching (Oxford Plasma-Therm 790 RIE system, 200 W, 10 min). The patterned PI thin film served as the encapsulation layer covering the whole interconnects except the electrode areas. Next, the sample was immersed in acetone for 12 h to fully dissolve the PMMA layer. Water soluble tapes (WSTs) were utilized as a stamp to pick up the prepared pattern. The receiving PDMS (Sylgard 184, Dow Corning Corporation, crosslink: PDMS = 1:20) substrates and the electronics attached WSTs were exposed to the UV induced ozone to create chemical groups between the electrodes and PDMS for enhancing the bonding strength[52] Tightly attaching the WSTs on the PDMS and then heated in an oven at 70 °C for 10 min formed strong bonding. Immersing the sample in water to remove the WSTs and realized soft stretchable electrodes. Next, the top PDMS layer (crosslink:PDMS = 1:10) was then spin-coated on top of the electrode. Suck air bubbles out of PDMS by vacuum pump for 20 min, then heat it at 120 °C for 1 min, forming a robust structure with strong interface bonding between different layers.

Characterizations: The open-circuit voltage was measured by a DAQ6510 data acquisition/multimeter system. The short-circuit current was calculated by measuring the voltage of a fixed value resistor which connected in series with the triboelectric nanogenerator (the voltage was measured by PL3516/P Powerlab 16/35, which owns much lower noise signal and higher sampling rate than the DAQ6510 multimeter system). Tests with a volunteer were performed with their full, informed consent.

Supporting Information

Supporting Information is available from the Wiley Online Library or from the author.

Acknowledgements

Y.L. and L.W. contributed equally to this work. This work was supported by City University of Hong Kong (Grant No. 9610423).

Conflict of Interest

The authors declare no conflict of interest.

Keywords

epidermal electronics, single-electrode structure, stretchable electronics, tactile sensing, triboelectric nanogenerators

Received: October 22, 2019
Published online: November 26, 2019

[1] J. Sun, A. Yang, C. Zhao, F. Liu, Z. Li, *Sci. Bull.* **2019**, *64*, 1336.
[2] H. Feng, C. Zhao, P. Tan, R. Liu, X. Chen, Z. Li, *Adv. Healthcare Mater.* **2018**, *7*, 1701298.
[3] K. Dong, X. Peng, Z. L. Wang, *Adv. Mater.* **2019**, *31*, 1902549.
[4] T. R. Ray, J. Choi, A. J. Bandodkar, S. Krishnan, P. Gutruf, L. Tian, R. Ghaffari, J. A. Rogers, *Chem. Rev.* **2019**, *119*, 5461.
[5] H. Liu, J. Zhong, C. Lee, S.-W. Lee, L. Lin, *Appl. Phys. Rev.* **2018**, *5*, 041306.
[6] K. Parida, J. Xiong, X. Zhou, P. S. Lee, *Nano Energy* **2019**, *59*, 237.
[7] X. Yu, T. J. Marks, A. Facchetti, *Nat. Mater.* **2016**, *15*, 383.
[8] K. Sim, Y. Gao, Z. Chen, J. Song, C. Yu, *Adv. Mater. Technol.* **2019**, *4*, 1800466.
[9] Y. Song, H. Chen, Z. Su, X. Chen, L. Miao, J. Zhang, X. Cheng, H. Zhang, *Small* **2017**, *13*, 1702091.
[10] B. Shao, Y. Liu, X. Zhuang, S. Hou, S. Han, X. Yu, J. Yu, *J. Mater. Chem. C* **2019**, *7*, 10196.
[11] X. Yu, J. Smith, N. Zhou, L. Zeng, P. Guo, Y. Xia, A. Alvarez, S. Aghion, H. Lin, J. Yu, *Proc. Natl. Acad. Sci. USA* **2015**, *112*, 3217.
[12] S. Xu, Z. Yan, K.-I. Jang, W. Huang, H. Fu, J. Kim, Z. Wei, M. Flavin, J. McCracken, R. Wang, *Science* **2015**, *347*, 154.
[13] Y. Su, X. Ping, K. J. Yu, J. W. Lee, J. A. Fan, B. Wang, M. Li, R. Li, D. V. Harburg, Y. Huang, *Adv. Mater.* **2017**, *29*, 1604989.
[14] K. Sim, Z. Rao, Z. Zou, F. Ershad, J. Lei, A. Thukral, J. Chen, Q.-A. Huang, J. Xiao, C. Yu, *Sci. Adv.* **2019**, *5*, eaav9653.
[15] J. Kim, A. Banks, H. Cheng, Z. Xie, S. Xu, K. I. Jang, J. W. Lee, Z. Liu, P. Gutruf, X. Huang, *Small* **2015**, *11*, 906.
[16] X. Ning, X. Yu, H. Wang, R. Sun, R. Corman, H. Li, C. M. Lee, Y. Xue, A. Chempakasseril, Y. Yao, Z. Zhang, H. Luan, Z. Wang, W. Xia, X. Feng, R. H. Ewoldt, Y. Huang, Y. Zhang, J. A. Rogers, *Sci. Adv.* **2018**, *4*, eaat8313.
[17] X. Ning, H. Wang, X. Yu, J. A. Soares, Z. Yan, K. Nan, G. Velarde, Y. Xue, R. Sun, Q. Dong, H. Luan, C. M. Lee, A. Chempakasseril, M. Han, Y. Wang, L. Li, Y. Huang, Y. Zhang, J. A. Rogers, *Adv. Funct. Mater.* **2017**, *27*, 1605914.
[18] T. Ray, J. Choi, J. Reeder, S. P. Lee, A. J. Aranyosi, R. Ghaffari, J. A. Rogers, *Curr. Opin. Biomed. Eng.* **2019**, *9*, 47.

[19] X. Han, K. J. Seo, Y. Qiang, Z. Li, S. Vinnikova, Y. Zhong, X. Zhao, P. Hao, S. Wang, H. Fang, *NPJ Flexible Electron.* **2019**, *3*, 9.
[20] K. J. Seo, Y. Qiang, I. Bilgin, S. Kar, C. Vinegoni, R. Weissleder, H. Fang, *ACS Nano* **2017**, *11*, 4365.
[21] Y. Huang, Z. Mu, P. Feng, J. Yuan, *J. Appl. Mech.* **2019**, *86*, 031011.
[22] C. Dagdeviren, P. Joe, O. L. Tuzman, K.-I. Park, K. J. Lee, Y. Shi, Y. Huang, J. A. Rogers, *Extreme Mech. Lett.* **2016**, *9*, 269.
[23] B. Meng, W. Tang, X. Zhang, M. Han, W. Liu, H. Zhang, *Nano Energy* **2013**, *2*, 1101.
[24] X.-S. Zhang, M.-D. Han, R.-X. Wang, B. Meng, F.-Y. Zhu, X.-M. Sun, W. Hu, W. Wang, Z.-H. Li, H.-X. Zhang, *Nano Energy* **2014**, *4*, 123.
[25] X. Cheng, B. Meng, X. Zhang, M. Han, Z. Su, H. Zhang, *Nano Energy* **2015**, *12*, 19.
[26] S. Li, J. Wang, W. Peng, L. Lin, Y. Zi, S. Wang, G. Zhang, Z. L. Wang, *Adv. Energy Mater.* **2017**, *7*, 1602832.
[27] Z. Liu, S. Zhang, Y. Jin, H. Ouyang, Y. Zou, X. Wang, L. Xie, Z. Li, *Semicond. Sci. Technol.* **2017**, *32*, 064004.
[28] Y. Chen, B. Lu, D. Ou, X. Feng, *Sci. China Phys., Mech. Astron.* **2015**, *58*, 594601.
[29] B. Lu, Y. Chen, D. Ou, H. Chen, L. Diao, W. Zhang, J. Zheng, W. Ma, L. Sun, X. Feng, *Sci. Rep.* **2015**, *5*, 16065.
[30] X. Chen, S. Xu, N. Yao, Y. Shi, *Nano Lett.* **2010**, *10*, 2133.
[31] K.-I. Park, S. Xu, Y. Liu, G.-T. Hwang, S.-J. L. Kang, Z. L. Wang, K. J. Lee, *Nano Lett.* **2010**, *10*, 4939.
[32] X. Yu, H. Wang, X. Ning, R. Sun, H. Albadawi, M. Salomao, A. C. Silva, Y. Yu, L. Tian, A. Koh, *Nat. Biomed. Eng.* **2018**, *2*, 165.
[33] G. Zhao, Y. Zhang, N. Shi, Z. Liu, X. Zhang, M. Wu, C. Pan, H. Liu, L. Li, Z. L. Wang, *Nano Energy* **2019**, *59*, 302.
[34] X. Pu, M. Liu, X. Chen, J. Sun, C. Du, Y. Zhang, J. Zhai, W. Hu, Z. L. Wang, *Sci. Adv.* **2017**, *3*, e1700015.
[35] B. Shi, Z. Liu, Q. Zheng, J. Meng, H. Ouyang, Y. Zou, D. Jiang, X. Qu, M. Yu, L. Zhao, *ACS Nano* **2019**, *13*, 6017.
[36] X.-S. Zhang, M.-D. Han, R.-X. Wang, F.-Y. Zhu, Z.-H. Li, W. Wang, H.-X. Zhang, *Nano Lett.* **2013**, *13*, 1168.
[37] Y. Zi, C. Wu, W. Ding, Z. L. Wang, *Adv. Funct. Mater.* **2017**, *27*, 1700049.
[38] Y. Song, X. Cheng, H. Chen, J. Huang, X. Chen, M. Han, Z. Su, B. Meng, Z. Song, H. Zhang, *J. Mater. Chem. A* **2016**, *4*, 14298.
[39] Y. Yang, H. Zhang, J. Chen, Q. Jing, Y. S. Zhou, X. Wen, Z. L. Wang, *ACS Nano* **2013**, *7*, 7342.
[40] Y. Yang, Y. S. Zhou, H. Zhang, Y. Liu, S. Lee, Z. L. Wang, *Adv. Mater.* **2013**, *25*, 6594.
[41] H. Askari, A. Khajepour, M. B. Khamesee, Z. Saadatnia, Z. L. Wang, *Nano Today* **2018**, *22*, 10.
[42] X. Wang, M. Que, M. Chen, X. Han, X. Li, C. Pan, Z. L. Wang, *Adv. Mater.* **2017**, *29*, 1605817.
[43] Z. Ren, J. Nie, J. Shao, Q. Lai, L. Wang, J. Chen, X. Chen, Z. L. Wang, *Adv. Funct. Mater.* **2018**, *28*, 1802989.
[44] U. Eduok, O. Faye, J. Szpunar, *Prog. Org. Coat.* **2017**, *111*, 124.
[45] L. Wang, W. A. Daoud, *Adv. Energy Mater.* **2019**, *9*, 1803183.
[46] Y. Yu, Z. Li, Y. Wang, S. Gong, X. Wang, *Adv. Mater.* **2015**, *27*, 4938.
[47] A. Diaz, R. Felix-Navarro, *J. Electrost.* **2004**, *62*, 277.
[48] L. Wang, X. Yang, W. A. Daoud, *J. Mater. Chem. A* **2018**, *6*, 11198.
[49] H. Ryu, J. H. Lee, T. Y. Kim, U. Khan, J. H. Lee, S. S. Kwak, H. J. Yoon, S. W. Kim, *Adv. Energy Mater.* **2017**, *7*, 1700289.
[50] Z. L. Wang, *Faraday Discuss.* **2015**, *176*, 447.
[51] J. Zhao, G. Zhen, G. Liu, T. Bu, W. Liu, X. Fu, P. Zhang, C. Zhang, Z. L. Wang, *Nano Energy* **2019**, *61*, 111.
[52] Y. Sun, J. A. Rogers, *J. Mater. Chem.* **2007**, *17*, 832.

